Molecular Crystals and Liquid Crystals
Publication details, including instructions for authors and subscription information:
http://www.tandfonline.com/loi/gmcl20

White Organic Light-Emitting Diodes With Different Order of RGB-Emitting Layers

Mei Meng [a], Wook Song [a], You-Hyun Kim [a], Sang-Youn Lee [b], Chul Gyu Jhun [a], Chang-Bum Moon [a], Richard Wood [c] & Woo-Young Kim [a b c]

[a] School of Display Engineering, Hoseo University, Beabang-Eup, Asan-City, Chungnam, South Korea

[b] Department of Semiconductor Display Engineering, Hoseo University, Beabang-Eup, Asan-City, Chungnam, South Korea

[c] Department of Engineering Physics, McMaster University, Hamilton, Ontario, Canada

Version of record first published: 16 Nov 2012.

To cite this article: Mei Meng , Wook Song , You-Hyun Kim , Sang-Youn Lee , Chul Gyu Jhun , Chang-Bum Moon , Richard Wood & Woo-Young Kim (2012): White Organic Light-Emitting Diodes With Different Order of RGB-Emitting Layers, Molecular Crystals and Liquid Crystals, 569:1, 125-142

To link to this article: http://dx.doi.org/10.1080/15421406.2012.694752

Mol. Cryst. Liq. Cryst., Vol. 569: pp. 125–142, 2012

ISSN: 1542-1406 print/1563-5287 online
DOI: 10.1080/15421406.2012.694752

Taylor & Francis
Taylor & Francis Group

White Organic Light-Emitting Diodes With Different Order of RGB-Emitting Layers

MEI MENG,[1] WOOK SONG,[1] YOU-HYUN KIM,[1] SANG-YOUN LEE,[2] CHUL GYU JHUN,[1] CHANG-BUM MOON,[1] RICHARD WOOD,[3] AND WOO-YOUNG KIM[1,2,3,*]

[1]School of Display Engineering, Hoseo University, Beabang-Eup, Asan-City, Chungnam, South Korea
[2]Department of Semiconductor Display Engineering, Hoseo University, Beabang-Eup, Asan-City, Chungnam, South Korea
[3]Department of Engineering Physics, McMaster University, Hamilton, Ontario, Canada

To achieve the emissive layers in white organic light-emitting diode (WOLED) for the three primary colors, DCJTB doped in Alq_3, C545T doped in Alq_3, and BCzVBi doped in MADN were applied for red, green, and blue emissive layer, respectively. By stacking all the red, green, and blue emissive layers in a single device, WOLED devices with the color coordinates close to (0.33, 0.33) were successfully fabricated. The structure of the blue–green–red (BGR) type of the three primary color WOLED device was NPB(700 Å)/MADN:BCzVBi-13%(210 Å)/Alq_3:C545T-2%(30 Å)/Alq_3:DCJTB-2%(60 Å)/Alq_3(300 Å)/Liq(20 Å)/Al(1000 Å). Its maximum luminance and luminous efficiency were 25,680 cd m^{-2} and 3.79 cd A^{-1}, as well as its white color coordinate was (0.32, 0.31) at 7 V. The structure of blue–red–green (BRG) type of the three primary color WOLED device was NPB(700 Å)/MADN:BCzVB-13%(210 Å)/Alq_3:DCJTB-2%(30 Å)/Alq_3: C545T-2%(60 Å)/Alq_3(300 Å)/Liq(20 Å)/Al(1000 Å). Its maximum luminance and luminous efficiency were 26,010 cd m^{-2} and 4.95 cd A^{-1}, as well as its white color coordinate was (0.33, 0.33) at 7 V. Both devices were successfully induced closer to the ideal white emissive lighting source, and three different peaks at 480 nm, 512 nm, and 616 nm could be confirmed at red, green, and blue region in electroluminescence (EL) spectra.

Keywords Different order; EML; three primary colors; WOLED

1. Introduction

Over the last 10 years, the performance of the white organic light-emitting diodes (WOLEDs) has steadily improved and attained a level requisite for acceptance into the backlights in liquid crystal displays and lighting market [1], hence, there is a greater appreciation for the potential of energy saving, thin, flexible WOLEDs to replace the traditional incandescent white light sources [2].

*Address correspondence to Woo-Young Kim, School of Display Engineering, Hoseo University, Beabang-Eup, Asan-City, Chungnam 336-795, South Korea; Tel.: 82-41-540-5944; Fax: 82-41-548-0650. E-mail: wykim@hoseo.edu

Ideally, the WOLED should have excellent properties of low driving voltage, high efficiency, light weight, bright emission, have Commission Internationale de L'eclairage (CIE) chromaticity coordinates of (0.33, 0.33), and a spectral response insensitive to drive current [3]. Nowadays, researchers throughout the world in both industry and academia are developing these WOLEDs for the next generation of solid-state light sources, and very recently the first products have become commercially available [4]. For the full color liquid crystal displays [5], the backlight unit (BLU) emitting the white light is required. Moreover, white light emission has drawn particular attention because any desired color range can be achieved by filtration of the white light [6,7]. For the application of the WOLED into the BLU of the liquid crystal display (LCD) panel and into the full color OLED, the WOLED emitting the three primary colors with high color purity is required.

It is the key issue in designing the WOLED with the multi-layer structure [8,9] that the spectrum of emission light from the layers emitting each primary color is balanced. In other words, an appropriate amount of the light intensity of each primary color is generated [10,11]. In this paper, to achieve the emissive layers in WOLED for the three primary colors, DCJTB doped in Alq_3, C545T doped in Alq_3, and BCzVBi doped in MADN were used for the red, green, and blue emissive layer, respectively. By stacking all the red, green, and blue emissive layers in a single device, WOLED devices with the high color purity were successfully fabricated with various thicknesses and in different orders of the red, green, and blue emission layers.

2. Experiment

Indium tin oxide (ITO)-coated glass was cleaned in the ultrasonic bath by the regular cleaning sequence: in the acetone, methanol, diluted water, and isopropyl alcohol. Hereafter, pre-cleaned ITO glass was treated by the O_2 plasma under the condition of 2×10^{-2} Torr, 125 W, and 2 min.

In the fabricated WOLED, N,N′-diphenyl-N,N′-bis(l-naphthyl-phenyl)-(l,l′-biphenyl)-4,4′-diamine(NPB) is used as hole transport layer (HTL), 2-methyl-9,10-di(2-naphthyl)anthracene (MADN) as blue host, 4,4′-(bis(9-ethyl-3-carbazovinylene)-1,1′-biphenyl(BCzVBi) as blue dopant, tris(8-hydroxyquinolino)-aluminum (Alq_3) as red and green host, 4-(dicyano-methylene)-2-t-butyle-6-(1,1,7,7-tetramethyl-julolidyl-9-enyl)-4H-pyran (DCJTB) as red dopant, 2,3,6,7-tetrahydro-1,1,7,7-tetramethyl-1H,5H,11H-10(2-benzothiazolyl)-quinolizine-[9,9a,1gh]coumarin (C545T) as a green dopant, Alq_3 as electron transport layer (ETL), and Liq as electron injection layer (EIL). Figure 1 shows the molecular structures of the organic materials used in the WOLED devices.

The organic and metal evaporations are conducted under the basic pressure of 8.0×10^{-7} Torr without breaking vacuum, and the evaporation rates were 1.0 Å s^{-1} for the organic materials of the HTL and ETL, 0.1 Å s^{-1} for the organic material of the EIL, and 5.0 Å s^{-1} for the metal. The doping concentration is adjusted by varying the relative evaporation speeds of the host and dopant materials, and the evaporation speeds are monitored with a quartz-oscillator thickness monitor.

With the direct current (DC) bias voltage, the optical and electrical properties of WOLEDs, such as the current density, luminance, luminous efficiency, CIE coordinates, and electroluminescence characteristics were measured by Keithley 238, CHROMA METER CS-100A, and JBS OLED analysis system IVL-200, respectively.

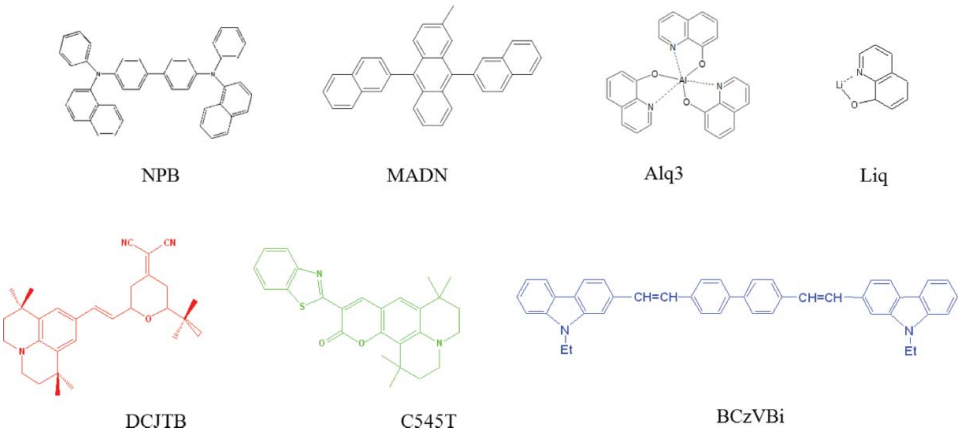

Figure 1. Molecular structures Alq_3 of organic materials in WOLEDs.

3. Results and Discussion

3.1 Photoluminescence and Absorption Spectrum of Emissive Materials in Host–Dopant System

Host–dopant system in WOLED is used to improve the electrical and optical performance, such as the color purity, current efficiency, and luminance of the host [12,13]. It is because at the same functional layer of the ETL or HTL, the Förster energy transfer [14] and the Dexter energy transfer [15], from the carrier transport layer to the host of the emissive layer, are different as compared with the energy transfer from host to dopant.

All the devices that were fabricated included fluorescence dopants. The fluorescence dyes can only utilize singlet states via the Förster energy transfer, which is a cause of the overlap between host fluorescence and dopant absorption spectra. So before fabricating the host–dopant devices, we had chosen the emissive materials according to the photoluminescence (PL) and absorption spectra considering the energy transfer efficiency.

Figure 2 shows the PL spectrum of Alq_3 at 516 nm, and absorption and PL spectra of the DCJTB at 502 nm and 601 nm, respectively. The PL spectrum of host Alq_3 and the absorption spectrum of dopant DCJTB were overlapped around 500 nm, and the emission peak of the DCJTB appeared at about 616 nm. Thus, this host–dopant system with Alq_3–DCJTB was chosen for the red emissive layer due to reasonable energy transfer.

Figure 3 shows the PL spectrum of Alq_3 at 516 nm, and the absorption and PL spectra of C545T at 467 nm and 509 nm, respectively. Alq_3 itself is the green emissive material that can generate the green light even without any green dopant, such as C545T. C545T has absorption spectrum at 467 nm with shorter wavelength than the PL spectrum of Alq_3 at 516 nm. The Förster energy transfer from Alq_3 to C545T is not so much expected, but if the doping concentration of C545T is sufficiently high, the distance between host and dopant molecules is close enough to induce the Förster energy transfer from Alq_3 to C545T. The highest occupied molecular orbital (HOMO) and lowest occupied molecular orbital (LUMO) energy levels of C545T are 5.6 eV and 3.1 eV, while those of Alq_3 are 5.8 eV and 3.2 eV, respectively. Therefore, it is probable that the electron and hole carriers are trapped in host–dopant interface due to the similar energy band gaps of Alq_3 and C545T.

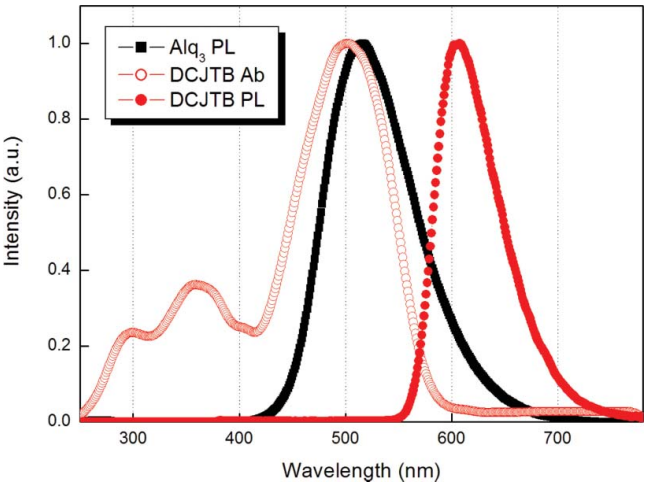

Figure 2. PL spectrum of Alq_3 and UV–Vis absorption and PL spectra of DCJTB.

Figure 4 shows the PL spectrum of MADN at 430 nm, and the absorption and PL spectra of BCzVBi at 392 nm and 462 nm, respectively. MADN is used for the blue emission layer even without BCzVBi, which is a blue dopant. BCzVBi shows the absorption spectrum at 392 nm with shorter wavelength than the PL spectrum of MADN at 430 nm. The Förster energy transfer from MADN to BCzVBi is more difficult to induce than Alq_3–C545T, but the energy level of MADN and BCzVBi is similar, and then the distance between molecules in host–dopant system is close enough to induce the Dexter energy transfer from MADN to BCzVBi by increasing the doping concentration of BCzVBi.

3.2 Electrical and Optical Characteristics of Mono Color OLED Devices

In order to combine the three primary colors for WOLED, we prepared the three kinds of the mono color OLED devices. It is not only good method for selecting the best doping

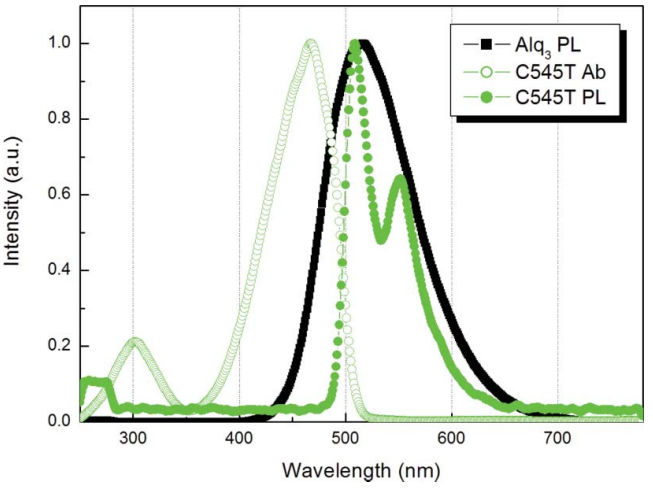

Figure 3. PL spectrum of Alq_3 and UV–Vis absorption and PL spectra of C545T.

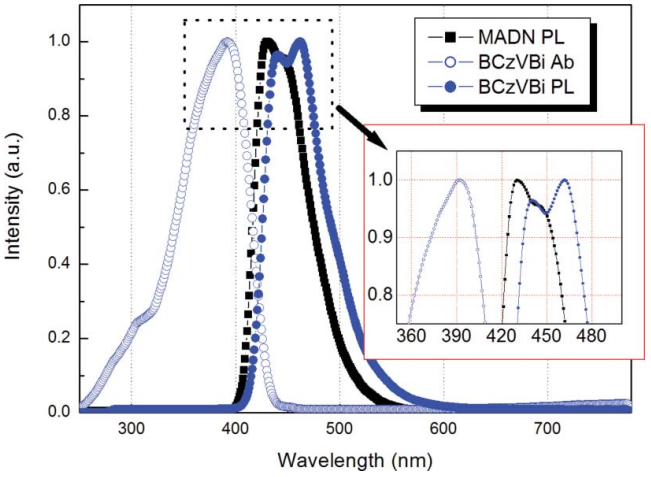

Figure 4. PL spectrum of MADN and UV–Vis absorption and PL spectra of BCzVBi.

concentration in each color, but also helpful to determine the optimized thickness of each emissive layer in WOLEDs in terms of the efficiency and luminance. Figure 5 shows the energy band diagram of the RGB mono color OLED devices.

The red emission devices A1–A4 with DCJTB doped in Alq_3 were fabricated with the total EML thickness of 300 Å and doping concentrations of 1.0%, 1.5%, 2.0%, and 2.5%, as shown in Table 1. The results of current–voltage–luminescence (*I–V–L*) characteristics were shown in Fig. 6. Electrical performances of these red OLED devices, such as current density, luminance, and luminous efficiency, decreased as the doping concentration increased. It was also confirmed that the red emission shifted to longer wavelengths in the energy-level (EL) spectra from 620 nm to 632 nm. This phenomenon could be explained by the interaction between dipole molecules due to the decrease of the distance between host and dopant molecules [16]. Although, the color purity and stability are important, efficiency and luminance also play an important role in the WOLED device. The lifetime of OLED device might also be decreased with high doping concentration. Thus, we selected the device of A3 with Alq_3:DCJTB-2.0% as a red emissive layer in three primary color WOLED devices. Table 2 summarized the performance of red OLED device with various doping concentrations.

Green emission devices B1–B5 with C545T doped in Alq_3 were fabricated with the total EML thickness of 300 Å and various doping concentrations of 0%, 1.0%, 1.5%, 2.0%, and 2.5%, as shown in Table 3. The electrical and optical performances of these

Table 1. Structures of red OLED devices A1–A4

Device	Structure
A1	NPB(700 Å)/Alq_3:DCJTB-1.0%(300 Å)/Alq_3(300 Å)/Liq(20 Å)/Al(1000 Å)
A2	NPB(700 Å)/Alq_3:DCJTB-1.5%(300 Å)/Alq_3(300 Å)/Liq(20 Å)/Al(1000 Å)
A3	NPB(700 Å)/Alq_3:DCJTB-2.0%(300 Å)/Alq_3(300 Å)/Liq(20 Å)/Al(1000 Å)
A4	NPB(700 Å)/Alq_3:DCJTB-2.5%(300 Å)/Alq_3(300 Å)/Liq(20 Å)/Al(1000 Å)

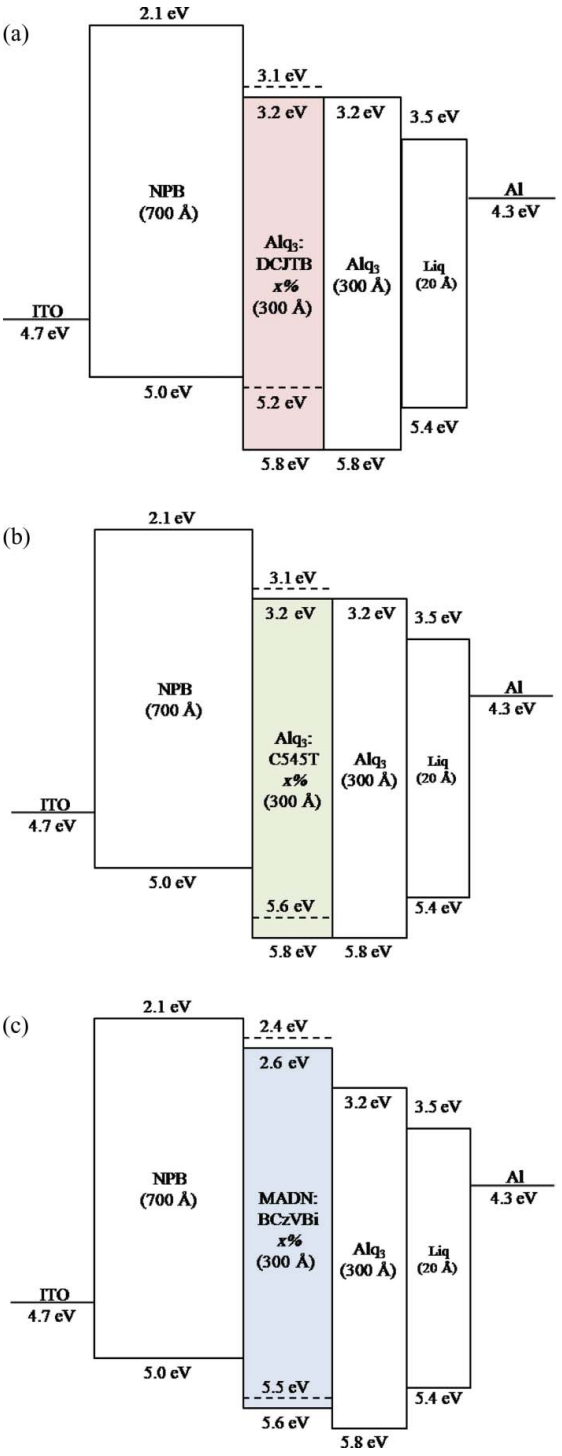

Figure 5. Energy band diagram of mono color OLED devices.

Table 2. Electrical and optical performances of device A

Device	Current density at 9 V (mA cm^{-2})	Luminance at 9 V (cd m^{-2})	Maximum luminous efficiency (cd A^{-1})	CIExy coordinates at 7 V
A1	55.29	2268	5.48	(0.61, 0.38)
A2	39.06	1180	4.41	(0.63, 0.37)
A3	27.51	664.3	3.85	(0.64, 0.35)
A4	23.62	486.8	3.17	(0.65, 0.35)

Table 3. Structures of green OLED devices B1–B5

Device	Structure
B1	NPB(700 Å)/Alq_3(300 Å)/Alq_3(300 Å)/Liq(20 Å)/Al(1000 Å)
B2	NPB(700 Å)/Alq_3:C545T-1.0%(300 Å)/Alq_3(300 Å)/Liq(20 Å)/Al(1000 Å)
B3	NPB(700 Å)/Alq_3:C545T-1.5%(300 Å)/Alq_3(300 Å)/Liq(20 Å)/Al(1000 Å)
B4	NPB(700 Å)/Alq_3:C545T-2.0%(300 Å)/Alq_3(300 Å)/Liq(20 Å)/Al(1000 Å)
B5	NPB(700 Å)/Alq_3:C545T-2.5%(300 Å)/Alq_3(300 Å)/Liq(20 Å)/Al(1000 Å)

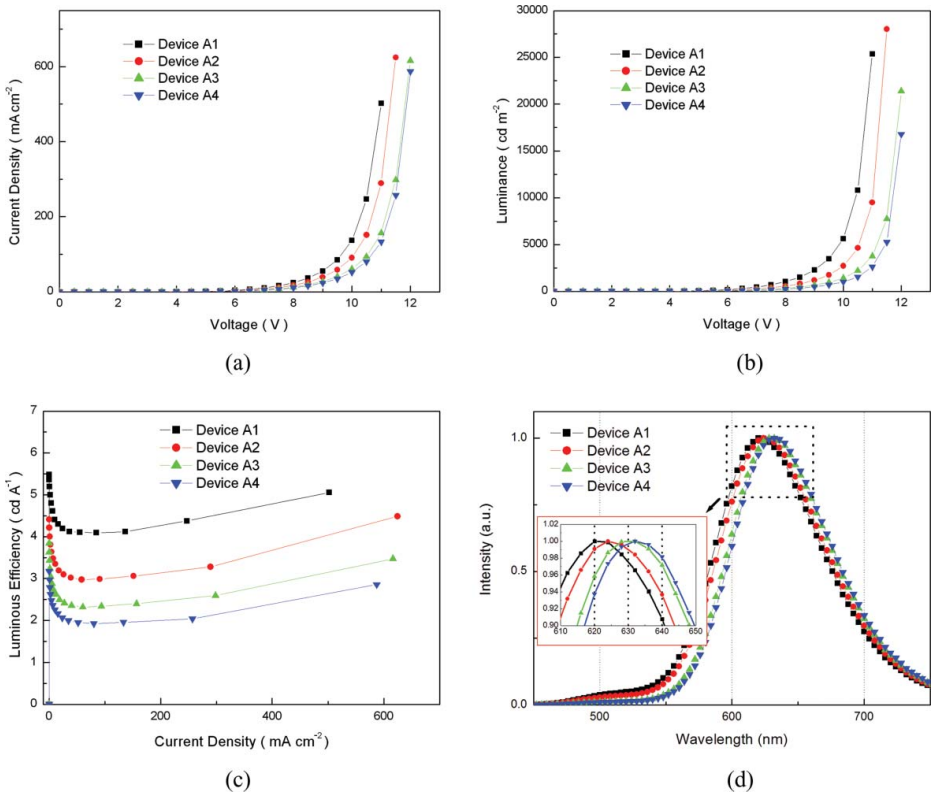

Figure 6. (a) Current densities of device A. (b) Luminance of device A. (c) Luminous efficiencies of device A. (d) EL spectra of device A.

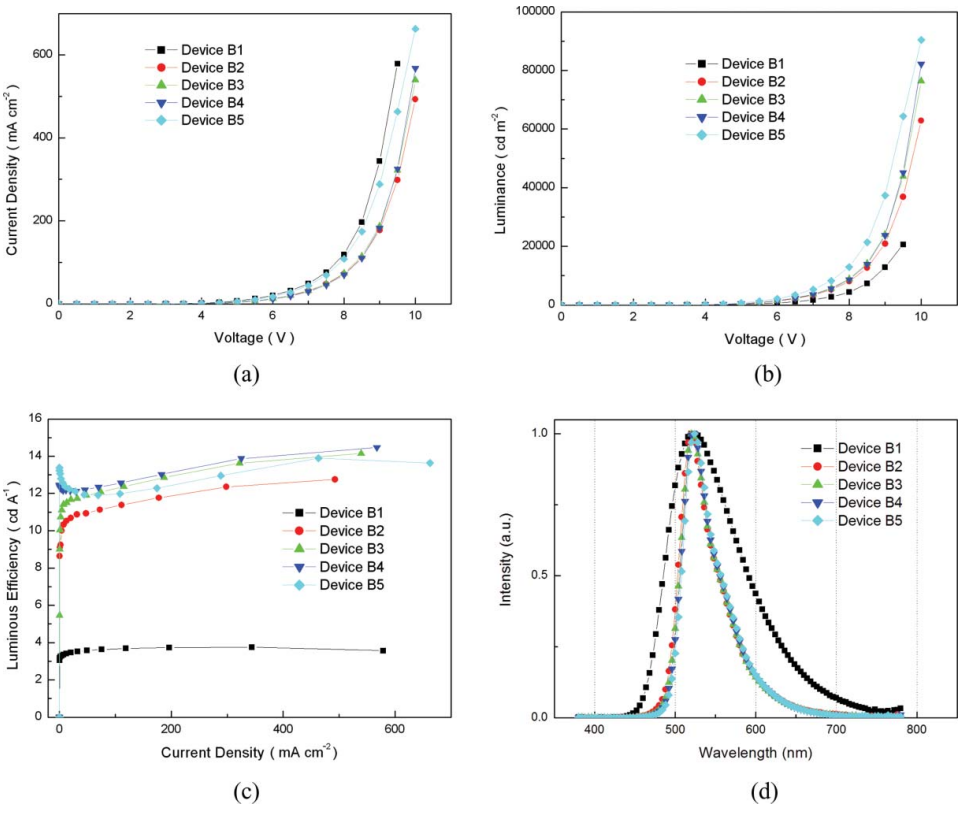

Figure 7. (a) Current densities of device B. (b) Luminance of device B. (c) Luminous efficiencies of device B. (d) EL spectra of device B.

green OLED devices were much better than those of blue and red mono color devices as shown in Fig. 7. As the doping concentration increased to 2.0% and 2.5%, concentration quenching happened. So, the optimal concentration of C545T could be obtained between 1.5% and 2.0%. As mentioned above, considering the Förster energy transfer from green and blue emissive layers to red emissive layer, in this work, we selected device B4 with Alq_3:C545T-2.0% as a green emissive layer in three primary color WOLED devices. The performance of green OLED devices B1–B5 is summarized in Table 4.

Table 4. Electrical and optical performances of device B

Device	Current density at 9 V (mA cm^{-2})	Luminance at 9 V (cd m^{-2})	Maximum luminous efficiency (cd A^{-1})	CIExy coordinates at 7 V
B1	343.80	12,880	3.74	(0.34, 0.55)
B2	177.69	20,910	12.75	(0.29, 0.64)
B3	187.21	24,070	14.15	(0.29, 0.65)
B4	182.45	23,760	14.47	(0.30, 0.65)
B5	288.35	37,340	13.64	(0.30, 0.65)

Table 5. Structures of blue OLED devices C1–C5

Device	Structure
C1	NPB(700 Å)/MADN(300 Å)/Alq_3(300 Å)/Liq(20 Å)/Al(1000 Å)
C2	NPB(700 Å)/MADN:BCzVBi-8%(300 Å)/Alq_3(300 Å)/Liq(20 Å)/Al(1000 Å)
C3	NPB(700 Å)/ MADN:BCzVBi-10%(300 Å)/Alq_3(300 Å)/Liq(20 Å)/Al(1000 Å)
C4	NPB(700 Å)/ MADN:BCzVBi-13%(300 Å)/Alq_3(300 Å)/Liq(20 Å)/Al(1000 Å)
C5	NPB(700 Å)/ MADN:BCzVBi-15%(300 Å)/Alq_3(300 Å)/Liq(20 Å)/Al(1000 Å)

Blue emission devices C1–C5 with BCzVBi doped in MADN were fabricated with the total EML thickness of 300 Å and various doping concentrations of 0%, 8%, 10%, 13%, and 15%, as shown in Table 5. Generally, molecular distance that allows the Förster energy transfer is about 100 Å, and concentration of dopant is about 1%–2%. However, the band gap of dopant BCzVBi is larger than that of the host of MADN, which is different from common host–dopant system. High doping concentrations were selected to reduce the distance between host and dopant molecules, which possibly generate the Dexter energy transfer. The electrical and optical performances with the host–dopant system were compared with those of non-doping device in Fig. 8. As the doping concentration is increased, the electrical

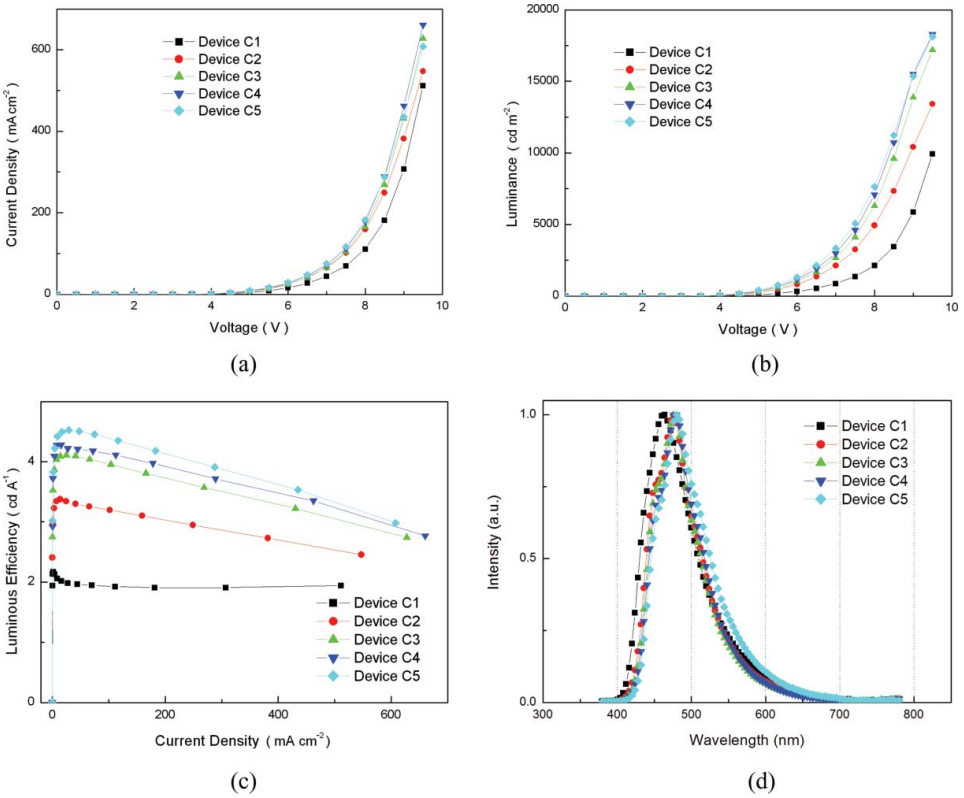

Figure 8. (a) Current densities of device C. (b) Luminance of device C. (c) Luminous efficiencies of device C. (d) EL spectra of device C.

Table 6. Electrical and optical performances of devices C1–C5

Device	Current density at 9 V (mA cm^{-2})	Luminance at 9 V (cd m^{-2})	Maximum luminous efficiency (cd A^{-1})	CIExy coordinates at 7 V
C1	307.01	5856	2.17	(0.18,0.21)
C2	381.61	10,410	3.37	(0.17,0.23)
C3	430.79	13,880	4.11	(0.17,0.23)
C4	462.30	15,490	4.28	(0.17,0.25)
C5	434.94	15,360	4.52	(0.17,0.26)

performances of these blue devices, such as current density, luminance, and luminous efficiency, decreased significantly at 13%. However, the emission spectra shifted to longer wavelength because of BCzVBi's emission in Alq_3. The LUMO level of MADN and BCzVBi are 2.6 eV and 2.4 eV, while that of Alq_3 is 3.2 eV. Therefore, all the excitons formed at the interface between emissive layer and the ETL cannot move to the BCzVBi layer, and some of them moved to the Alq_3 layer. It was implied that the probability of the energy transfer to Alq_3 was depended on the concentration of BCzVBi as the dopant. So, we selected device C4 with MADN:BCzVBi-13% as a blue emissive layer in three primary color WOLED devices. Table 6 summarized the performance of blue OLED devices C1–C5.

Figure 9 compares EL of device C5 and device D whose structure is NPB(700 Å)/MADN: BCzVBi-15%(300 Å)/Bphen(300 Å)/Liq(20 Å)/Al(1000 Å). 4,7-Diphenyl-1,10-phenanthroline (Bphen) used in device D is a non-emissive ETL material. As shown in Fig. 9, 518 nm peak intensities of device C5 appeared in green region was stronger than that of device D, while BCzVBi's blue emissive peaks can be found at 460 and 480 nm

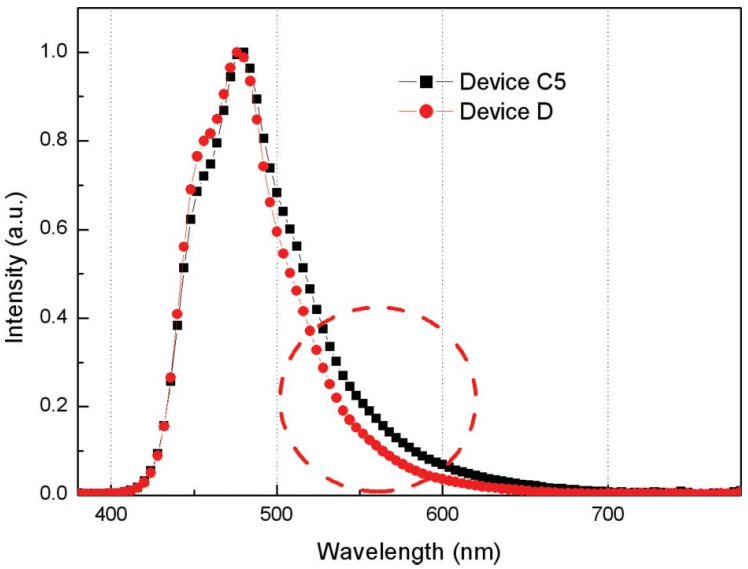

Figure 9. EL spectra of device C5 and device D.

Table 7. Structures of the WOLED devices W1 to W2

Device	Structure
W1-1	NPB(700 Å)/MADN(220 Å)/Alq_3(60 Å)/Alq_3:DCJTB-2.0%(20 Å)/Alq_3 (300 Å)/Liq(20 Å)/Al(1000 Å)
W1-2	NPB(700 Å)/MADN(220 Å)/Alq_3(50 Å)/Alq_3:DCJTB-2.0%(30 Å)/Alq_3 (300 Å)/Liq(20 Å)/Al(1000 Å)
W2-1	NPB(700 Å)/MADN(220 Å)/Alq_3:DCJTB-2.0%(20 Å)/Alq_3(60 Å)/Alq_3 (300 Å)/Liq(20 Å)/Al(1000 Å)
W2-2	NPB(700 Å)/MADN(220 Å)/Alq_3:DCJTB-2.0%(10 Å)/Alq_3(70 Å)/Alq_3 (300 Å)/Liq(20 Å)/Al(1000 Å)
W2-3	NPB(700 Å)/MADN(200 Å)/Alq_3:DCJTB-2.0%(10 Å)/Alq_3(90 Å)/Alq_3 (300 Å)/Liq(20 Å)/Al(1000 Å)

[17–20]. As a result, 15% of the BCzVBi is not suitable for the blue emissive layer with a drop in color purity.

3.3 WOLED Devices with DCJTB Doped Red Emissive Layer

To achieve white emission in OLEDs, the best mixing method of the three primary colors or two complement colors is required. In this experiment, three primary colors, such as blue, green, and red, were used to generate the white emission for white organic light-emitting devices. Because MADN and Alq_3 can render blue and green emission each, we focused on DCJTB for red emission in this section. The energy band diagrams of the WOLED devices W1 and W2 with DCJTB doped red emissive layer are shown in Fig. 10, and structure of the WOLED devices W1 and W2 are described in Table 7.

Figure 11(a)–(d) shows the current density, luminescence, luminous efficiency, EL spectra, and color coordinates of devices W1 and W2. As summarized in Table 8, the color coordinates of W1-1, 1-2, 2-1, 2-2, and 2-3 are (0.33, 0.31), (0.34, 0.31), (0.37, 0.30), (0.34, 0.30), and (0.35, 0.31), respectively, which are in the region of color coordinates for white emission as (0.33, 0.33)% ± 10%. However, these were changed significantly according to the order of emissive layers despite using same emission.

Figure 11(a) shows the *J–V* curves of devices W1 and W2. Current density of device W2-3 with 200 Å of the MADN thickness was the highest among all the devices. In contrast, devices W1-1 and W1-2 whose thickness of MADN was 220 Å show the lowest current

Table 8. Electrical and optical performances of device W1 and W2

Device	Current density at 9 V (mA cm^{-2})	Luminance at 9 V (cd m^{-2})	Maximum luminous efficiency (cd A^{-1})	CIExy coordinates at 7 V
W1-1	222.35	6026	3.89	(0.33,0.31)
W1-2	224.77	5921	4.02	(0.34,0.31)
W2-1	254.06	7515	4.29	(0.37,0.30)
W2-2	305.45	9294	3.98	(0.34,0.30)
W2-3	404.33	13,650	4.19	(0.35,0.31)

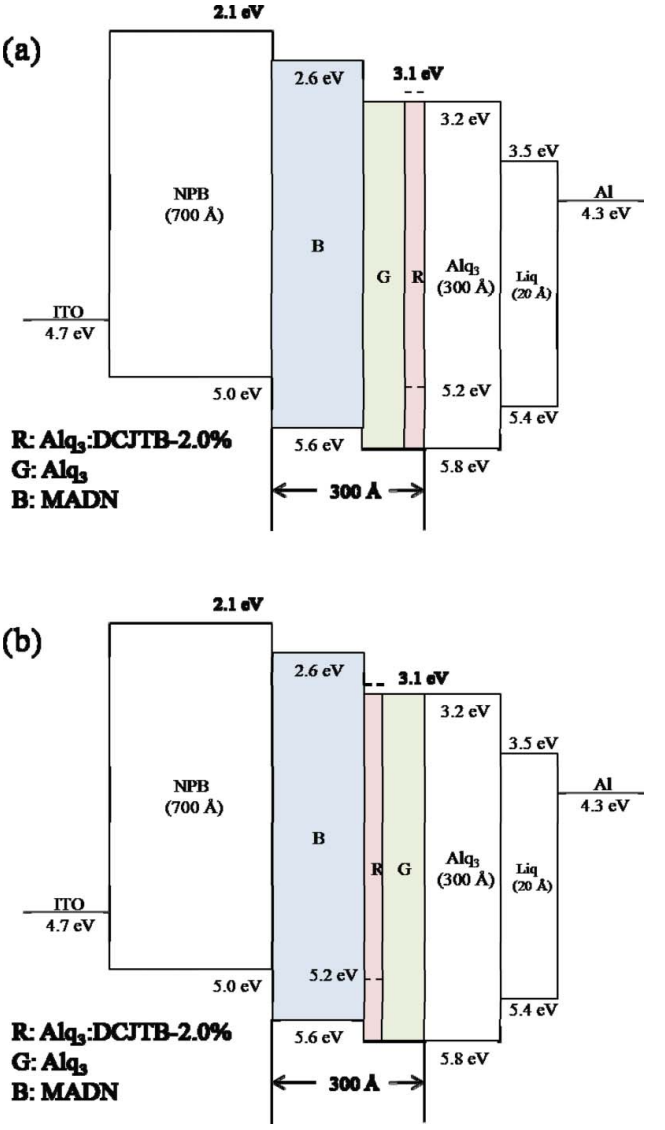

Figure 10. Energy band diagrams of the WOLED device W1(a) and W2(b).

density. Moreover, it can be found that current density of devices W1-1 and W1-2 whose red emissive layer located beside the ETL was almost identical, while current density of devices W2-1 and W2-2 whose red emissive layer located between the blue and green EML was depend on the thickness of the emissive layer. It can be seen that exciton formation occurred actively when DCJTB was placed between the blue and green EML, than when it was placed beside the ETL, and current density was greatly changed according to the thickness of the emissive layer. *L–V* curves in Fig. 11(b) as well as luminous efficiency in Fig. 11(c) show the similar tendency. The red emissive layer located right after the ETL, interfered flow of the electrons because the electrons were trapped in the Alq_3 layer due

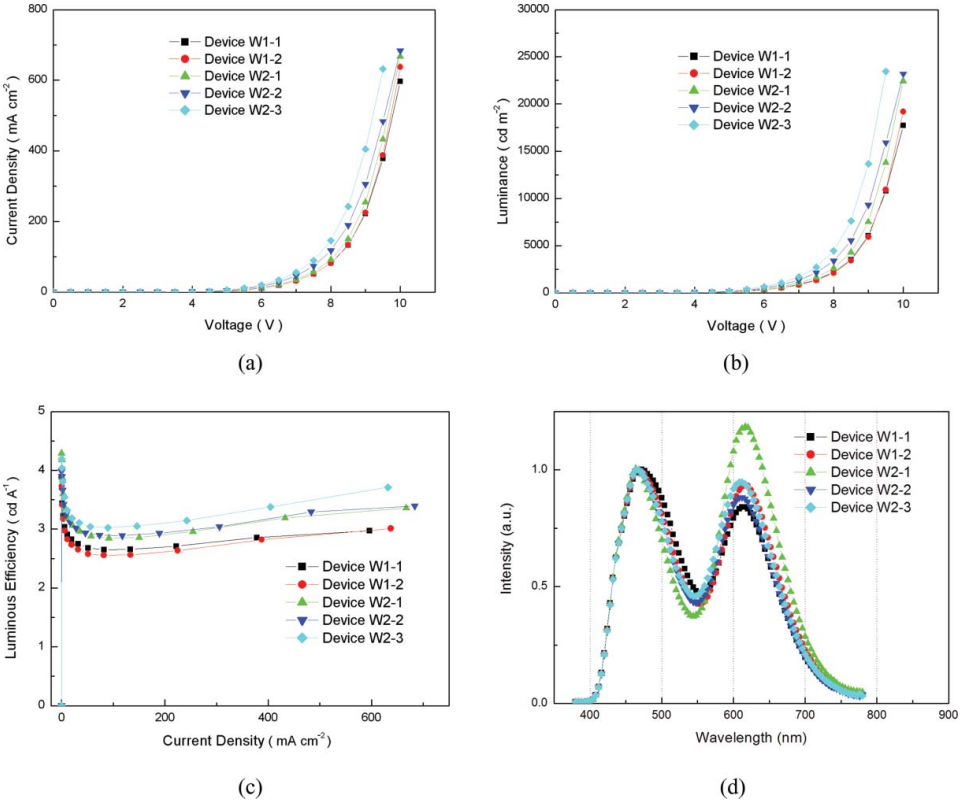

Figure 11. (a) Current densities of device W1 and W2. (b) Luminance of device W1 and W2. (c) Luminous efficiencies of device W1 and W2. (d) EL spectra of device W1 and W2.

to the low LUMO energy level of DCJTB, and then balance of electron and hole injection was lost.

3.4 WOLED Devices with RGB Doped Emissive Layers

Three primary color WOLEDs with DCJTB doped red EML have been fabricated. In order to improve the performance of WOLEDs, we then added BCzVBi and C545T into blue and green emissive layers as dopant materials. All the fabricated WOLED devices were listed in Table 9, as device W3 were BGR type, and W4 were BRG type according to the order of RGB emissive layers between HTL and ETL. Figure 12 shows the energy band diagrams of the WOLED devices W3 and W4.

Figure 13(a)–(d) shows the electrical and optical characteristics of the WOLED devices designing emitting layers in an order of blue, green, and red. Table 10 summarized the performance of WOLEDs W3 with the thickness of BGR emissive layers accommodated, that color coordinates of devices W3-1, 3-2, 3-3, and 3-4 were (0.37, 0.33), (0.35, 0.33), (0.32, 0.30), and (0.32, 0.31), respectively. All of the devices were available in the range of white color coordinates (0.33, 0.33)% $\pm$ 10%.

As shown in Fig. 13(a), current densities of devices W3-1 and W3-2 decreased as the red emissive layer was getting thicker. Being different from the WOLED devices only in the

Table 9. Structures of the WOLED devices W3 and W4

Device	Structure
W3-1	NPB(700 Å)/MADN:BCzVBi-13%(200 Å)/Alq_3:C545T-2.0% (20 Å)/Alq_3:DCJTB-2.0%(80 Å)/Alq_3(300 Å)/Liq(20 Å)/Al(1000 Å)
W3-2	NPB(700 Å)/MADN:BCzVBi-13%(200 Å)/Alq_3:C545T-2.0% (30 Å)/Alq_3:DCJTB-2.0%(70 Å)/Alq_3(300 Å)/Liq(20 Å)/Al(1000 Å)
W3-3	NPB(700 Å)/MADN:BCzVBi-13%(210 Å)/Alq_3:C545T-2.0% (20 Å)/Alq_3:DCJTB-2.0%(70 Å)/Alq_3(300 Å)/Liq(20 Å)/Al(1000 Å)
W3-4	NPB(700 Å)/MADN:BCzVBi-13%(210 Å)/Alq_3:C545T-2.0% (30 Å)/Alq_3:DCJTB-2.0%(60 Å)/Alq_3(300 Å)/Liq(20 Å)/Al(1000 Å)
W4-1	NPB(700 Å)/MADN:BCzVBi-13%(200 Å)/Alq_3:DCJTB-2.0% (40 Å)/Alq_3:C545T-2.0%(60 Å)/Alq_3(300 Å)/Liq(20 Å)/Al(1000 Å)
W4-2	NPB(700 Å)/MADN:BCzVBi-13%(200 Å)/Alq_3:DCJTB-2.0% (50 Å)/Alq_3:C545T-2.0%(50 Å)/Alq_3(300 Å)/Liq(20 Å)/Al(1000 Å)
W4-3	NPB(700 Å)/MADN:BCzVBi-13%(210 Å)/Alq_3:DCJTB-2.0% (30 Å)/Alq_3:C545T-2.0%(60 Å)/Alq_3(300 Å)/Liq(20 Å)/Al(1000 Å)
W4-4	NPB(700 Å)/MADN:BCzVBi-13%(210 Å)/Alq_3:DCJTB-2.0% (40 Å)/Alq_3:C545T-2.0%(50 Å)/Alq_3(300 Å)/Liq(20 Å)/Al(1000 Å)

red-doped emissive layer, the device of W3-2 had a higher current density than that of the device of W3-4, even though the red emissive layer of the device of W3-2 was thicker than that of the device of W3-4. The same tendency can be seen in luminance performance of the device of W3 in Fig. 13(b). In addition, a great difference can be seen in luminous efficiency as the thickness of C545T changed, which is shown in Fig. 13(c). It can be described by that the luminous efficiency and luminance performance of the green emissive layer are much better than those of the blue and red emissive layers. Figure 13(d), which represents the EL spectra of the device of W3, shows that the intensity of the green at 512 nm and red at 616 nm from the device of W3-1 and W3-2 is higher than those of devices W3-3 and W3-4. It can be implied that emission region beside the HTL has a higher intensity than that beside the ETL, because the blue emission layer thickness of W3-1 and W3-2 was 200 Å, while that of W3-3 and W3-4 was 210 Å.

Figure 14(a)–(d) shows the electrical and optical characteristics of the WOLED devices designing emitting layers in an order of blue, red, and green. Table 11 summarized the performance of WOLEDs, W4 with the thickness of BGR emissive layers accommodated that color coordinates of devices W4-1, 4-2, 4-3, and 4-4 were (0.36, 0.34), (0.37, 0.33),

Table 10. Electrical and optical performances of device W3

Device	Current density at 9 V (mA cm^{-2})	Luminance at 9 V (cd m^{-2})	Maximum luminous efficiency (cd A^{-1})	CIExy coordinates at 7 V
W3-1	140.68	4453	3.74	(0.37,0.33)
W3-2	368	13,340	4.20	(0.35,0.33)
W3-3	252.72	8264	3.79	(0.32,0.30)
W3-4	278.57	9893	3.97	(0.32,0.31)

Table 11. Electrical and optical performances of device W4

Device	Current density at 9 V (mA cm^{-2})	Luminance at 9 V (cd m^{-2})	Maximum luminous efficiency (cd A^{-1})	CIExy coordinates at 7 V
W4-1	181.45	7442	4.48	(0.36,0.35)
W4-2	183.39	6832	4.44	(0.37,0.34)
W4-3	272.34	12,330	4.95	(0.33,0.33)
W4-4	301.56	12,340	4.67	(0.33,0.31)

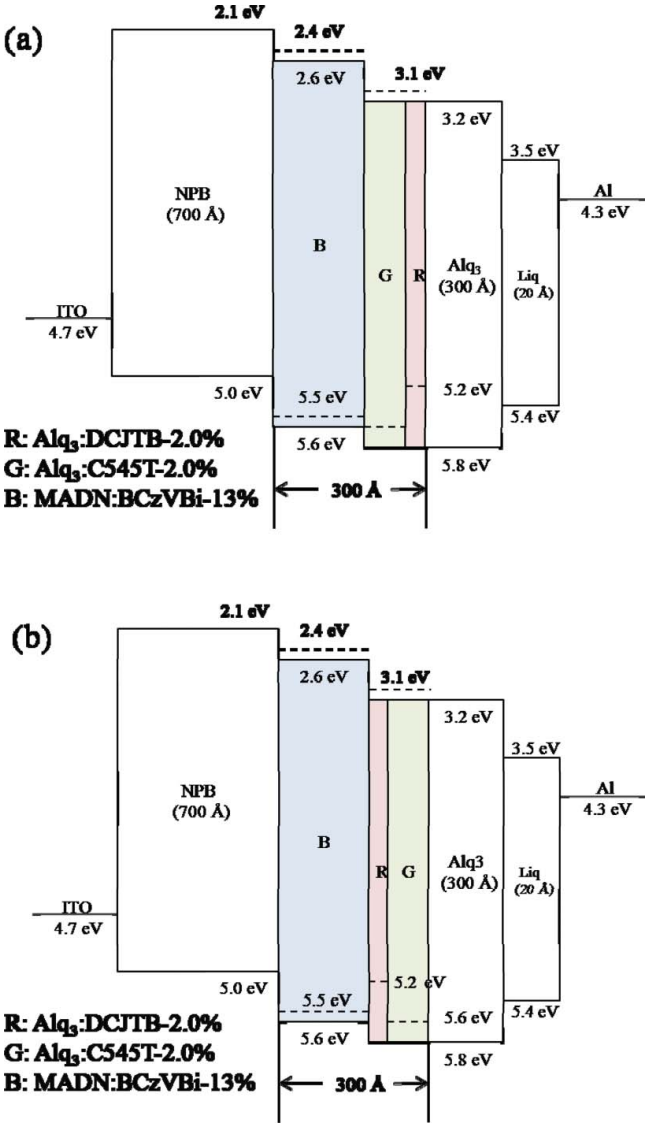

Figure 12. Energy band diagram of the WOLED device W3(a) and W4(b).

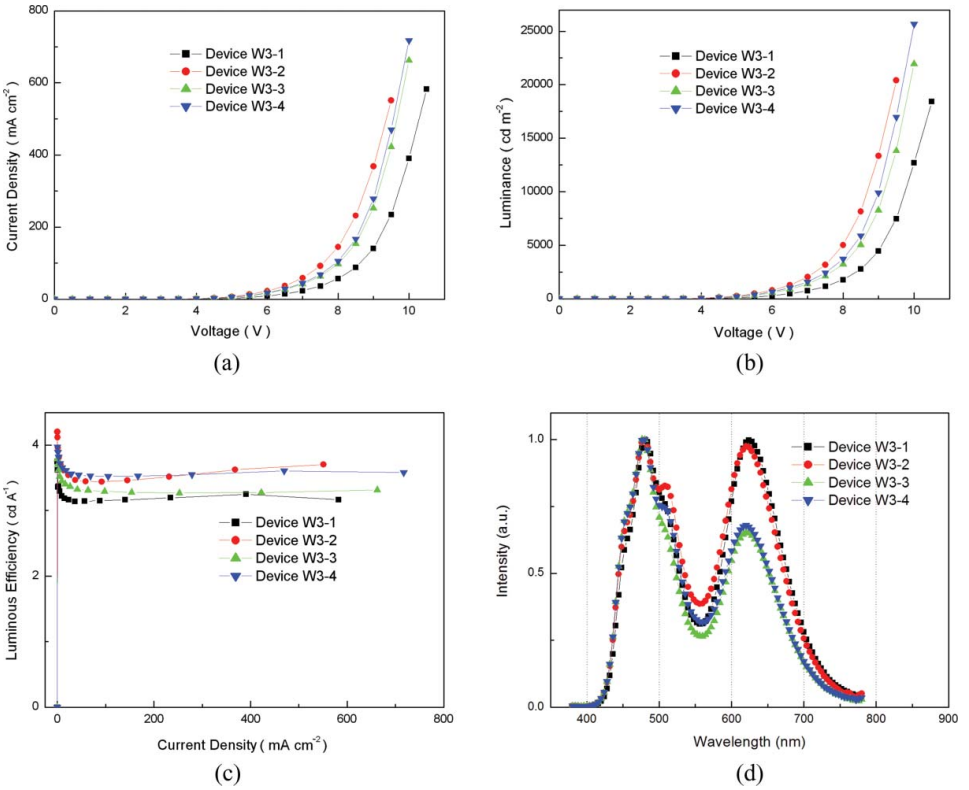

Figure 13. (a) Current densities of device W3. (b) Luminance of device W3. (c) Luminous efficiencies of device W3. (d) EL spectra of device W3.

(0.32, 0.33), and (0.32, 0.31), respectively. All of the devices were available in the range of white color coordinates (0.33, 0.33)% ± 10%.

As shown in Fig. 14(a), current densities of W4 increased as the blue emissive layer was getting thicker, which was different from BGR WOLED device of W3. Similar tendency can be observed in luminance performance of the device of W4 in Fig. 14(b). Being different from BGR type WOLEDs, red emissive layer in BRG type WOLEDs, which has the smallest band gap located between those of blue and green emissive layers. The recombination between the electron and hole occurred at the interface of MADN and Alq_3, and most of the energy transfer happened to DCJTB in the red emissive layer. Therefore, the current density and luminance performance of the device of W4 greatly changed when the red emissive layer was located between blue and green emissive layers.

However, the luminous efficiency of the device W4 in Fig. 14(c) shows the better performance as the thickness of green emission become larger, which was the same tendency as that of the BGR type device of W3. It is because the green emissive layer has significantly better performance of the current efficiency and luminance than the blue and red emissive layers.

As shown in Fig. 14(d), the devices of W4-1 and W4-2 whose blue emissive layer were 200 Å, red emission peaks at 616 nm have a great difference, while the devices of W4-3 and W4-4 whose blue emissive layer were 210 Å, the 616 nm red emission peaks have nearly no difference as the thickness of the red emission layer changed. It proved that the

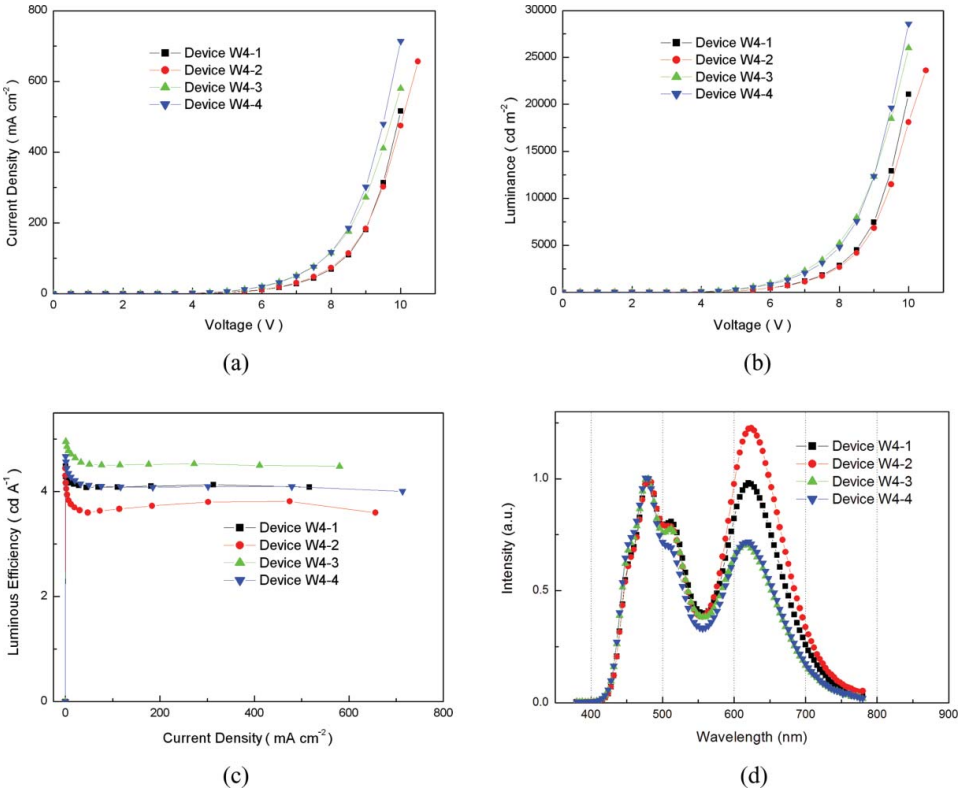

Figure 14. (a) Current densities of device W4. (b) Luminance of device W4. (c) Luminous efficiencies of device W4. (d) EL spectra of device W4.

probability of the recombination between the electron and hole is high when the thickness of the EML is 210 Å as mentioned previously.

4. Conclusion

Three primary color WOLED used for the display application have been fabricated to improve the electrical and optical performance, such as the color purity, current efficiency, and luminance. BRG type WOLED devices in which red emissive layer with the smallest band gap located at the central position had a better performance than BGR type WOLED. The recombination of electron and hole occurred at the interface of MADN and Alq_3, and most of the energy transfer happened to DCJTB in the red emission layer. Luminous efficiency of WOLEDs with three primary colors using MADN as host material was 3.20 cd A^{-1} [21]. The results obtained in this paper are useful for the OLED scientists and engineers as WOLED's current efficiency of 4.95 cd A^{-1} is 50% higher than previous literatures as well as the color purity of the WOLED devices was successfully induced closer to the ideal white emissive lighting source of (0.33, 0.33). The electro-optical performance of WOLED can be improved and optimized by changing the order of blue, red, and green emission layers with various phosphorescence dopants in future research.

Acknowledgment

This research was supported by the Research Fund of Korean Academia-Industry Collaboration (San-Hak Hyubdong) Foundation (10-105) in 2010.

References

[1] Duggal, R., Shiang, J. J., Heller, C. M., & Foust, D. F. (2002). *Appl. Phys. Lett.*, *80*, 3470.
[2] D'Andrade, B. W., & Forrest, S. R. (2004). *Adv. Mater. (Weinheim, Germany)*, *16*, 1585.
[3] Deshpande, R. S., Bulovic, V., & Forrest, S. R. (1999). *Appl. Phys. Lett.*, *75*, 888.
[4] Kido, J., Hongawa, K., Okuyama, K., & Nagai, K. (1994). *Appl. Phys. Lett.*, *64*, 815.
[5] Adachi, C., Baldo, M. A., Forrest, S. R., Lamansky, S., Thompson, M. E., & Kwong, R. C. (2001). *Appl. Phys. Lett.*, *78*, 622.
[6] Strukeji, M., Jordan, R. H., & Dodabalapur, A. (1996). *J. Am. Chem. Soc.*, *118*, 1213.
[7] Zhang, Z. L., Jiang, X. Y., Zhu, W. Q., Zhang, B. X., & Xu, S. H. (2001). *J. Phys. D: Appl. Phys.*, *34*, 3083.
[8] Lei, G. T., Wang, L. D., & Qiu, Y. (2004). *Appl. Phys. Lett.*, *85*, 5403.
[9] Kido, J., Ikeda, W., Kimura, M., & Nagai, K. (1996). *Jpn. J. Appl. Phys. Part 2*, *35*, L394.
[10] Jiang, X.-Y., Zhang, Z.-L., Zhu, W.-Q., & Xu, S.-H. (2006). *Displays*, *27*, 161.
[11] Chu, H. Y., Lee, J.-I., & Do, L.-M. (2003). *Mol. Cryst. Liq. Cryst.*, *405*, 119.
[12] Adachi, C., Baldo, M. A., Thompson, M. E., & Forrest, S. R. (2001). *J. Appl. Phys.*, *90*, 5048.
[13] Wen, S. W., Lee, M. T., & Chen, C. H. (2005). *J. Display Technol.*, *1*, 90.
[14] Lakowicz, J. R. (1991). *Topics in Fluorescence Spectroscopy, vol.. 2*, Plenum: New York.
[15] Pope, M., & Swenberg, C. E. (1999). *Electronic Processes in Organic Crystals and Polymers,* 2nd ed., vol. 1, Oxford University Press: New York.
[16] Zhang, F. J., Xu, Z., Zhao, D. W., Zhao, S. L., Wang, L. W., & Yuan, G. C. (2008). *Phys. Scr.*, *77*, 055403.
[17] Song, W., Meng, M., Kim, Y. H., Moon, C. B., Jhun, C. G., Lee, S. Y., Wood, R., & Kim, W. Y. (2012). *J. Lumin.*, *132*, 2122.
[18] Sun, Y., Giebink, N. C., Kanno, H., Ma, B., Thompson, M. E., & Forrest, S. R. (2006). *Nature*, *440*, 908.
[19] Divayana, Y., Liu, S., Kyaw, A. K. K., & Sun, X. W. (2011). *Org. Electron.*, *12*, 1.
[20] Seo, J. H., Lee, S. C., Kim, Y. K., & Kim, Y. S. (2009). *Mol. Cryst. Liq. Cryst.*, *507*, 316.
[21] Meng, M., Kim, Y. H., Lee, S. Y., Song, W., Yang, H. J., Kim, G. W., Lee, B. M., Yu, H. H., Lee, C. K., & Kim, W. Y. (2011). *Nanosci. Nanotechnol. Lett.*, *3*, 131.